Supporting Information

Tuning SF_6 Affinity via Engineering Pore Environments in Metal–Organic Frameworks

Jackson Geary,[†a] Caith E. McKeown,[†a] Nickolas J. Gantzler,[a] N. Scott Bobbitt,[a] and Dorina F. Sava Gallis[a*]

[†]Co-first author

[a]Nanoscale Sciences Department, Sandia National Laboratories, Albuquerque, NM 87185, United States

*Corresponding Author: dfsava@sandia.gov

1. General Materials and Methods.

All chemicals, reagents and solvents, were purchased from commercial suppliers and used without alteration or further purification.

Powder X-ray diffraction measurements were performed on a Bruker D2Phaser instrument using CuKα radiation (λ = 1.54178 Å).

FT-iR spectra were collected on a Thermo Scientific Nicolet iS20 FTIR spectrometer with a Smart iTX diamond ATR.

Prior to gas sorption, samples were activated at 85 °C under vacuum for 12 h. N_2 adsorption isotherms were collected at 77.35 K and 298.15 K on a micromeritics ASAP 2020 surface area and porosity analyzer using ultra-high purity nitrogen (99.999%, obtained from Matheson Tri-Gas). CO_2 adsorption isotherms were collected at 298.15 K on the same instrument using research purity CO_2 (99.999%, obtained from Matheson Tri-Gas). Adsorption data were analyzed using Micromeritics Microactive software.

Thermogravimetric analysis (TGA) was conducted on a TA SDTQ600 instrument. Activated MOF samples were heated to 900 °C at a ramp rate of 10 °C per min^{-1} under continuous flow of air.

^{1}H NMR spectra were obtained on a 500 MHz Bruker Advance II Spectrometer and analyzed using Bruker Topspin software. ^{1}H NMR spectra were referenced to residual deuterated solvent peaks. Quantification of functional groups was performed by integrating relative to the singlet for trimesic acid.

Scanning electron microscopy (SEM) samples were prepared on a carbon taped SEM stub and sputter coated with Au or Pd prior to imaging. SEM images were collected using an FEI Verios 5 UC instrument at accelerating voltages between 2-10 kV. Energy dispersive X-ray spectroscopy (EDX) data were collected at 18 kV using an Ametek EDAX Octane Elite Super 70 mm EDX system.

2. Materials Synthesis.

2.1 Synthesis of MOF-808.

The synthesis of MOF-808 followed a modified literature procedure.[1, 2] Trimesic acid (0.210g, 1.00 mmol) and zirconyl chloride octahydrate (0.970 g, 3.01 mmol) were added to a 250 mL screw-top jar with a PTFE-lined lid. 30 mL of N,N-dimethylformamide (DMF) and 30 mL of formic acid were then added to dissolve the solids, and the mixture was heated to 100 °C in an isothermal oven for 24 h. The resulting white powder was collected and washed with DMF (3 x 30 mL) over 24 h, then washed with acetone (3 x 30 mL) over 24 h. The product was dried in a vacuum oven at 85 °C for 12 h. All characterization data consistent with previous literature reports.

2.2 General synthesis of fluorinated MOF-808.

MOF-808 (150 mg) and fluorinated reagent (3.30 mmol) were added to a 50 mL screw-top jar with a PTFE-lined lid. 25 mL of DMF was then added to the jar and sonicated to dissolve the

reagent. The mixture was heated in an isothermal oven to 60 °C for 18 h. The resulting white powder was collected and washed with DMF (3 x 30 mL) over 24 h, then washed with acetone (3 x 30 mL) over 24 h. The product was dried in a vacuum oven at 85 °C for 12 h.

2.2.1 Synthesis of MOF-808-F_1. MOF-808 (150 mg) and 4-flurobenzoic acid (462.3 mg, 3.30 mmol) were added to a 50 mL screw-top jar with PTFE-lined lid. 25 mL of DMF was then added to the jar and sonicated to dissolve the reagent. The mixture was heated in an isothermal oven to 60 °C for 18 h. The resulting white powder was collected and washed with DMF (3 x 30 mL) over 24 h, then washed with acetone (3 x 30 mL) over 24 h. The product was dried in a vacuum oven at 85 °C for 12 h. The success of incorporation was confirmed with digestion NMR and infrared spectroscopy.

2.2.2 Synthesis of MOF-808-F_2. MOF-808 (150 mg) and 4,5-diflurobenzoic acid (521.7 mg, 3.30 mmol) were added to a 50 mL screw-top jar with PTFE-lined lid. 25 mL of DMF was then added to the jar and sonicated to dissolve the reagent. The mixture was heated in an isothermal oven to 60 °C for 18 h. The resulting white powder was collected and washed with DMF (3 x 30 mL) over 24 h, then washed with acetone (3 x 30 mL) over 24 h. The product was dried in a vacuum oven at 85 °C for 12 h. The success of incorporation was confirmed with digestion NMR and infrared spectroscopy.

2.2.3 Synthesis of MOF-808-CF_3. MOF-808 (150 mg) and 4-(trifluoromethyl)benzoic acid (627.4 mg, 3.30 mmol) were added to a 50 mL screw-top jar with PTFE-lined lid. 25 mL of DMF was then added to the jar and sonicated to dissolve the reagent. The mixture was heated in an isothermal oven to 60 °C for 18 h. The resulting white powder was collected and washed with DMF (3 x 30 mL) over 24 h, then washed with acetone (3 x 30 mL) over 24 h. The product was dried in a vacuum oven at 85 °C for 12 h. The success of incorporation was confirmed with digestion NMR and infrared spectroscopy.

2.2.4 Synthesis of MOF-808-$(CF_3)_2$. MOF-808 (150 mg) and 3,5-bis(trifluoromethyl)benzoic acid (851.8 mg, 3.30 mmol) were added to a 50 mL screw-top jar with PTFE-lined lid. 25 mL of DMF was then added to the jar and sonicated to dissolve the reagent. The mixture was heated in an isothermal oven to 60 °C for 18 h. The resulting white powder was collected and washed with DMF (3 x 30 mL) over 24 h, then washed with acetone (3 x 30 mL) over 24 h. The product was dried in a vacuum oven at 85 °C for 12 h. The success of incorporation was confirmed with digestion NMR and infrared spectroscopy.

3. Computational methods

3.1 In Silico Functionalization

The in-silico functionalization procedure started with the MOF-808 structure and deployed PoreMatMod.jl[3] to identify formate groups on the Zr_6-nodes and sequentially swap these out with the desired moiety (e.g. F_1, F_2, CF_3, or $(CF_3)_2$). The sequential functionalization continues until the desired level of functionalization is achieved, or it is not possible to insert another functional group without incurring atomic overlap.

3.2 Density Functional Theory

DFT calculations were done in VASP v 6.4.2[4] using standard projector-augmented wave (PAW) pseudopotentials with an energy cutoff of 520 eV. Exchange-correlation was treated with the Perdew-Burke-Ernzerhof (PBE)[5] density functional and D3 dispersion corrections with Becke-Johnson damping.[6] Integration was treated using a 2x2x2 kpoint grid with Gaussian smearing and sigma value of 0.01. Geometric optimization used an SCF convergence criterion of 1.0e-5 with a force optimization criterion of 0.05 eV/Å. Charge calculations used a tighter SCF criterion of 1.0e-6. Partial charges were computed using the DDEC6 method implemented in the Chargemol program.[7-10]

3.3 GCMC Simulations

We used the RASPA (v. 2.0) software package[11, 12] to carry out Grand-Canonical Monte Carlo (GCMC) simulations at 298K over a pressure range from 0.1-100,000 Pa. Each simulation used 100,000 initialization and 100,000 production MC cycles -- where a cycle is defined as the greater of either 20 Monte Carlo moves or N, where N is number of adsorbate molecules in the system -- with allowable adsorbate moves and associated relative probabilities: swap (insertion and deletion, 0.25), rotation (0.25), translation (0.25), and reinsertion (0.25). To prevent molecules from occupying regions that would be physically prohibited, we used blocking spheres calculated in Zeo++[13, 14] using a probe radius of 1.82 Å (kinetic radius of N_2) and 50,000 samples.

Atomic pair-wise interactions are modeled using a 12-6 Lennard-Jones (LJ) and Coulombic potential with Lorentz-Berthelot mixing rules and a cutoff radius of 12.8 Å. The long-range Coulombic interactions, past the cutoff radius, are handled using the EWALD method. The MOF was replicated so that the minimum distance along any crystal axis exceeded twice the cutoff radius. During the simulations, the MOF atoms were held fixed with partial charges obtained from DFT, and the Lennard-Jones parameters obtained from the Universal Force Field.[15] We used the Martito-Marto force field parameters for SF_6.[16]

4. Tables and figures.

Table S1 shows the minimum, maximum, and average partial charge on F atoms computed using DFT and the DDEC6 partial charge method in Chargemol. Notably F atoms on the aromatic ring tend to have weaker charges than F atoms on a methyl group. We attribute this to the stronger electronegativity of the ring due to resonance. Also, we note that we have observed that equilibration methods like QEq tend to place too much charge on F atoms on aromatic rings likely due to underestimating the aromatic resonance and we recommend using DFT for charges for fluorinated structures.

Table S1 |Minimum, maximum, and average partial charges for F atoms in MOFs. Computed using DFT.

MOF	Min	Max	Avg
MOF-808-F_1	-0.166	-0.158	-0.162
MOF-808-F_2	-0.151	-0.148	-0.150
MOF-808-CF_3	-0.231	-0.209	-0.220
MOF-808-$(CF_3)_2$	-0.236	-0.196	-0.219

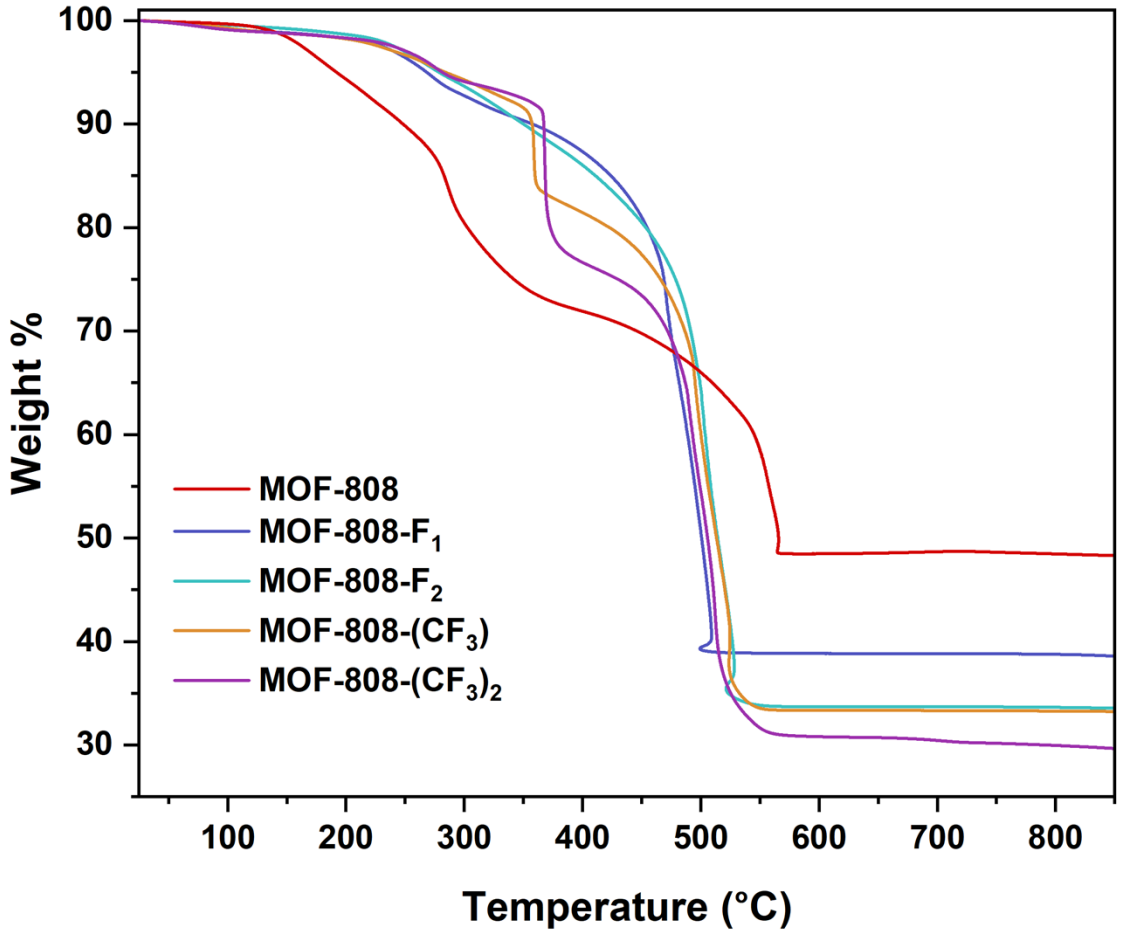

Figure S1 | TGA data for fluorinated MOF-808 materials under air.

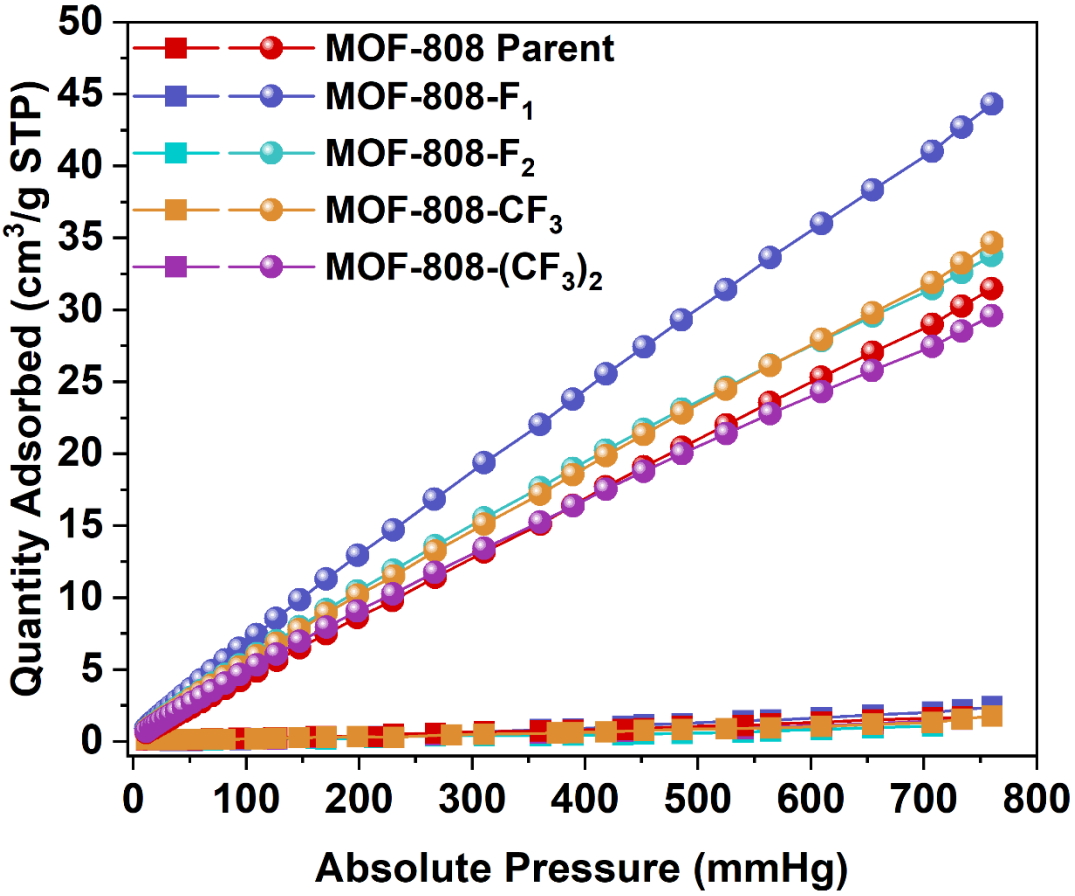

Figure S2 | CO_2 (filled spheres) and N_2 adsorption (filled squares) at 298K for parent MOF-808 and fluorinated MOF-808 materials.

Figure S3 | ^1H NMR spectrum of MOF-808-F_1 digested in KOD/D_2O.

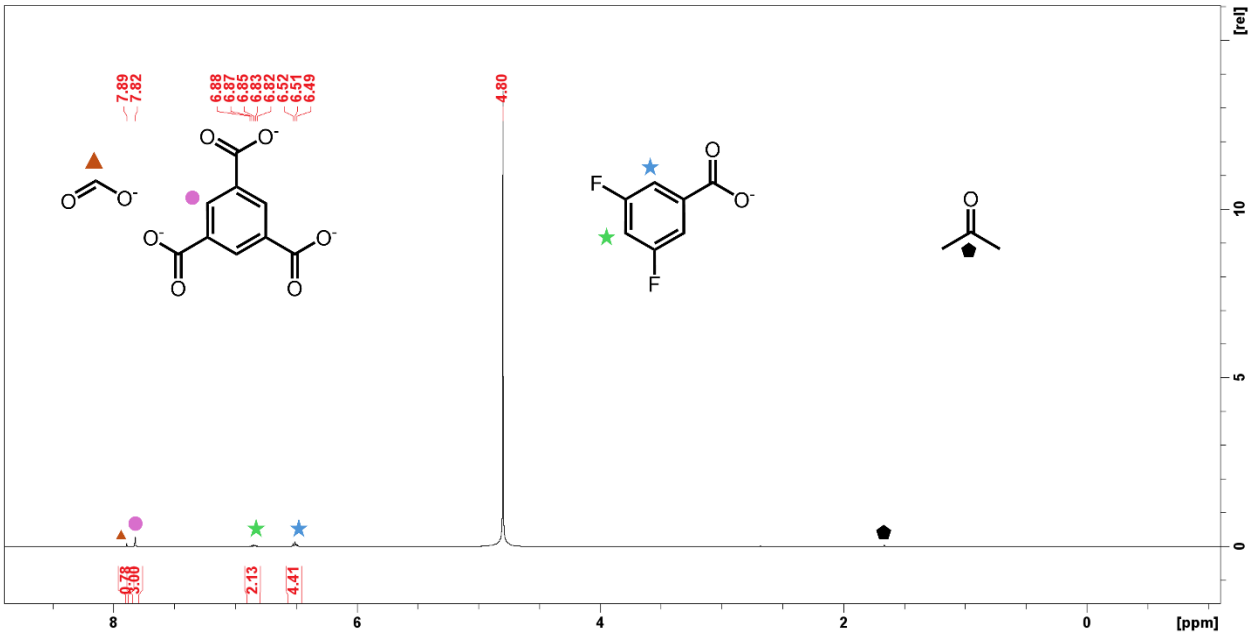

Figure S4 | ^{1}H NMR spectrum of MOF-808-F_2 digested in KOD/D_2O.

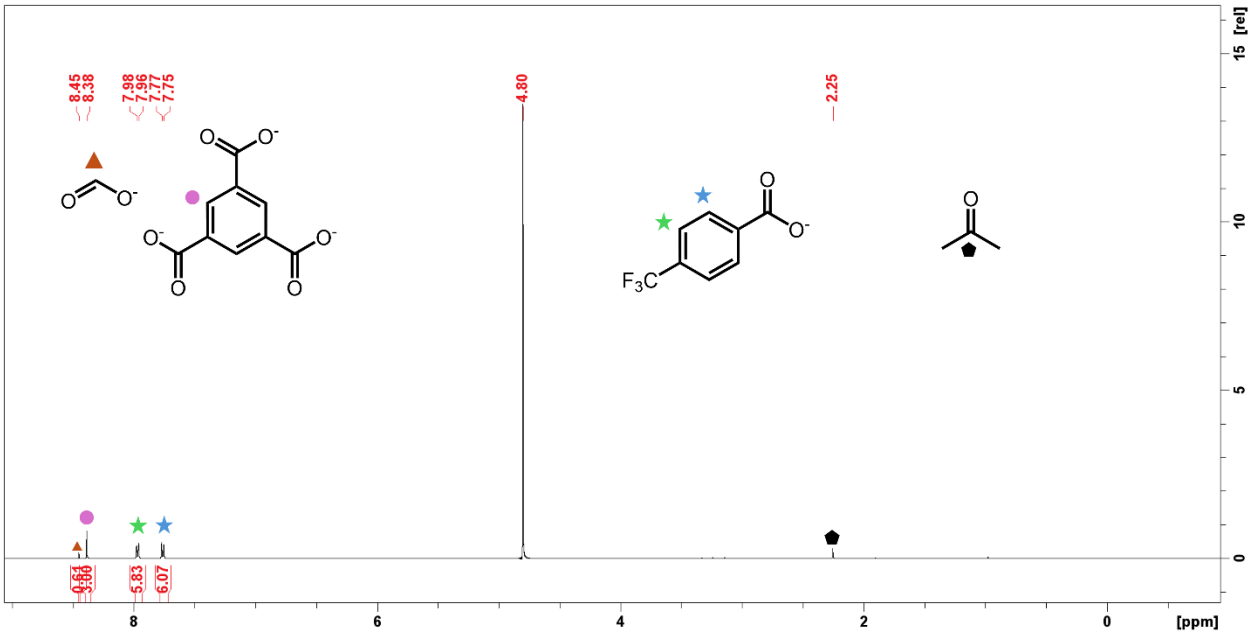

Figure S5 | ^{1}H NMR spectrum of MOF-808-CF_3 digested in KOD/D_2O.

Figure S6 | ^{1}H NMR spectrum of MOF-808-$(CF_3)_2$ digested in KOD/D_2O.

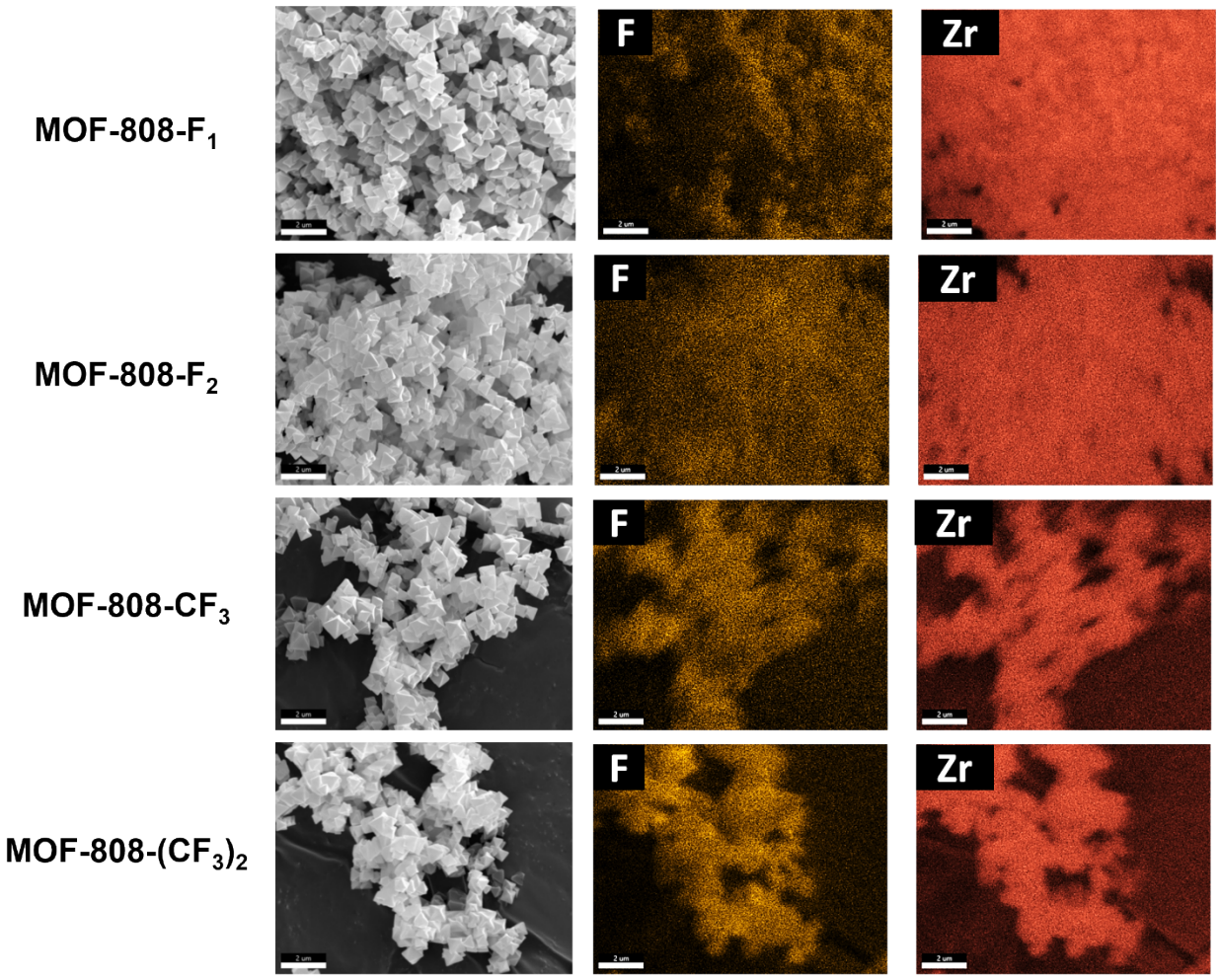

Figure S7 | SEM-EDS maps for the fluorinated MOF-808 materials.

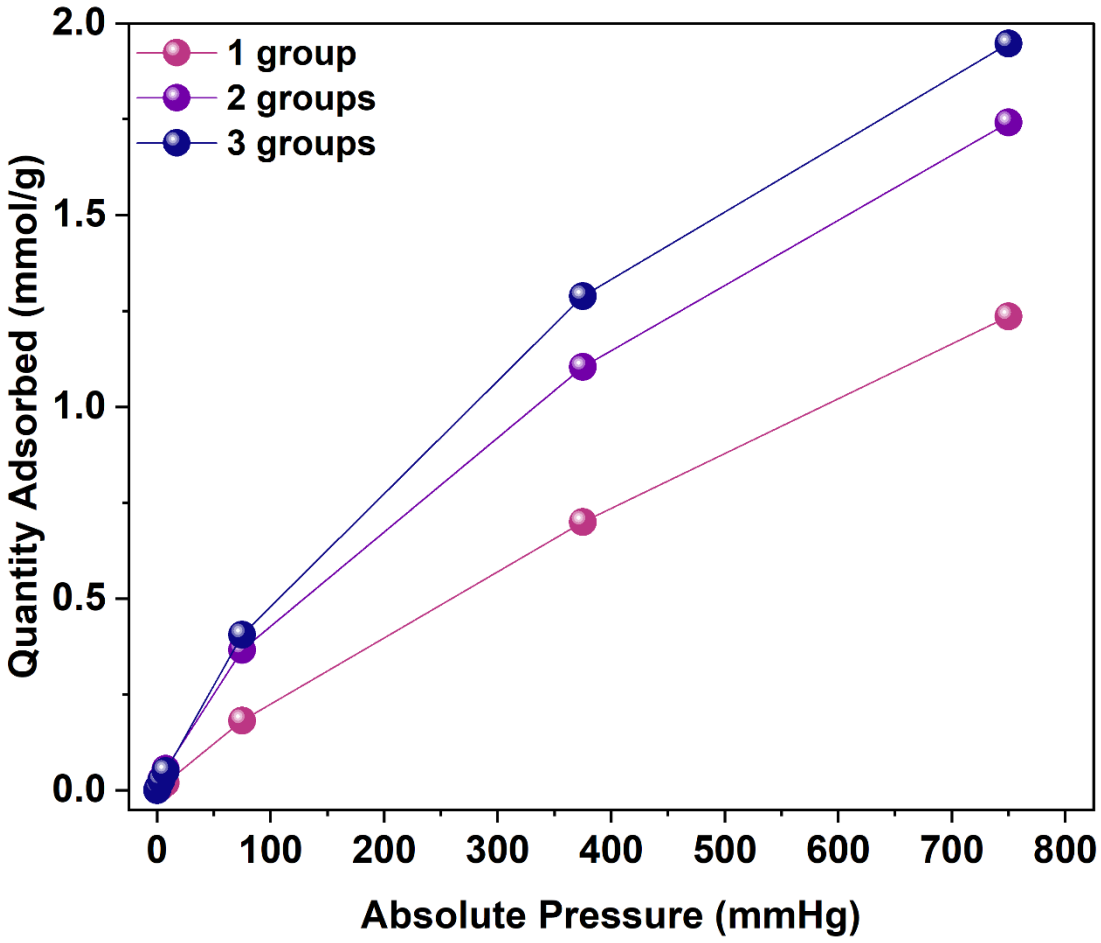

Figure S8 | Simulated SF_6 adsorption isotherms for MOF-808-F_1 at various functional group loadings.

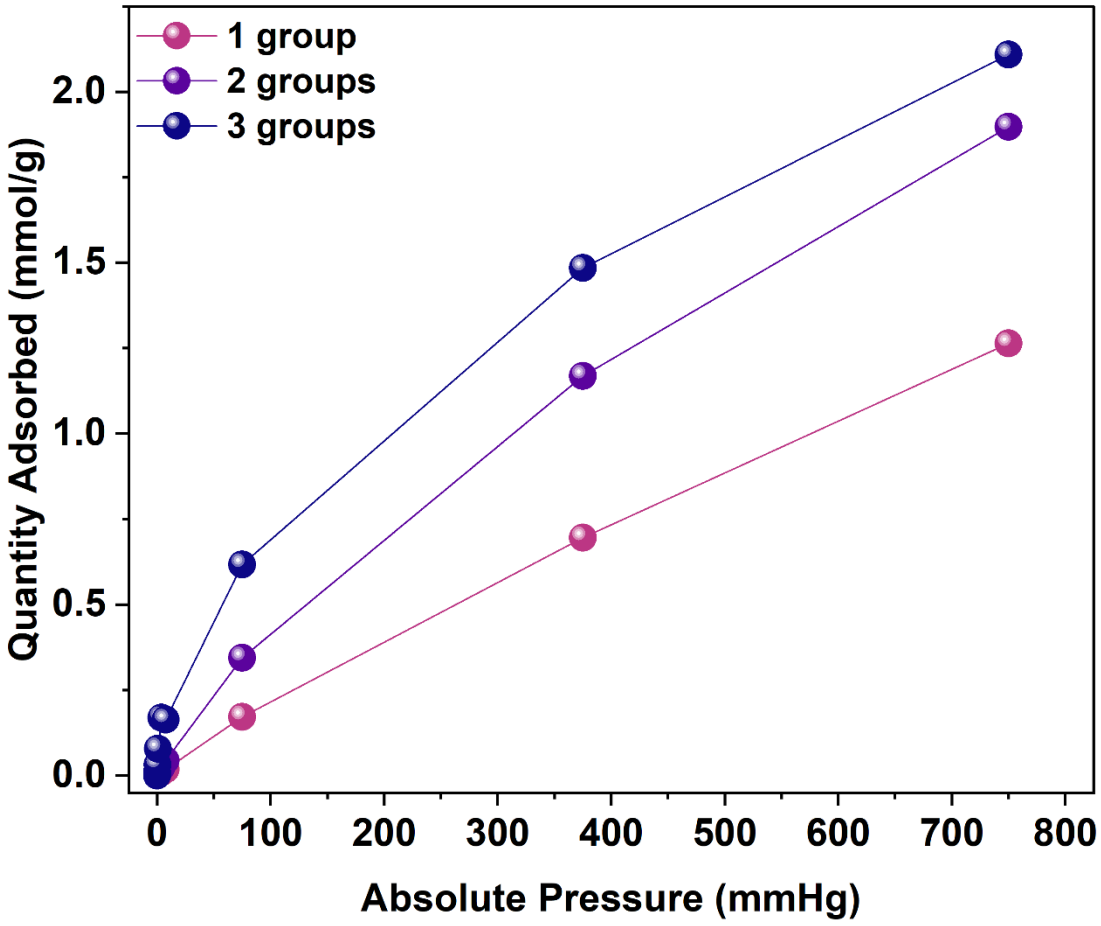

Figure S9 | Simulated SF_6 adsorption isotherms for MOF-808-F_2 at various functional group loadings.

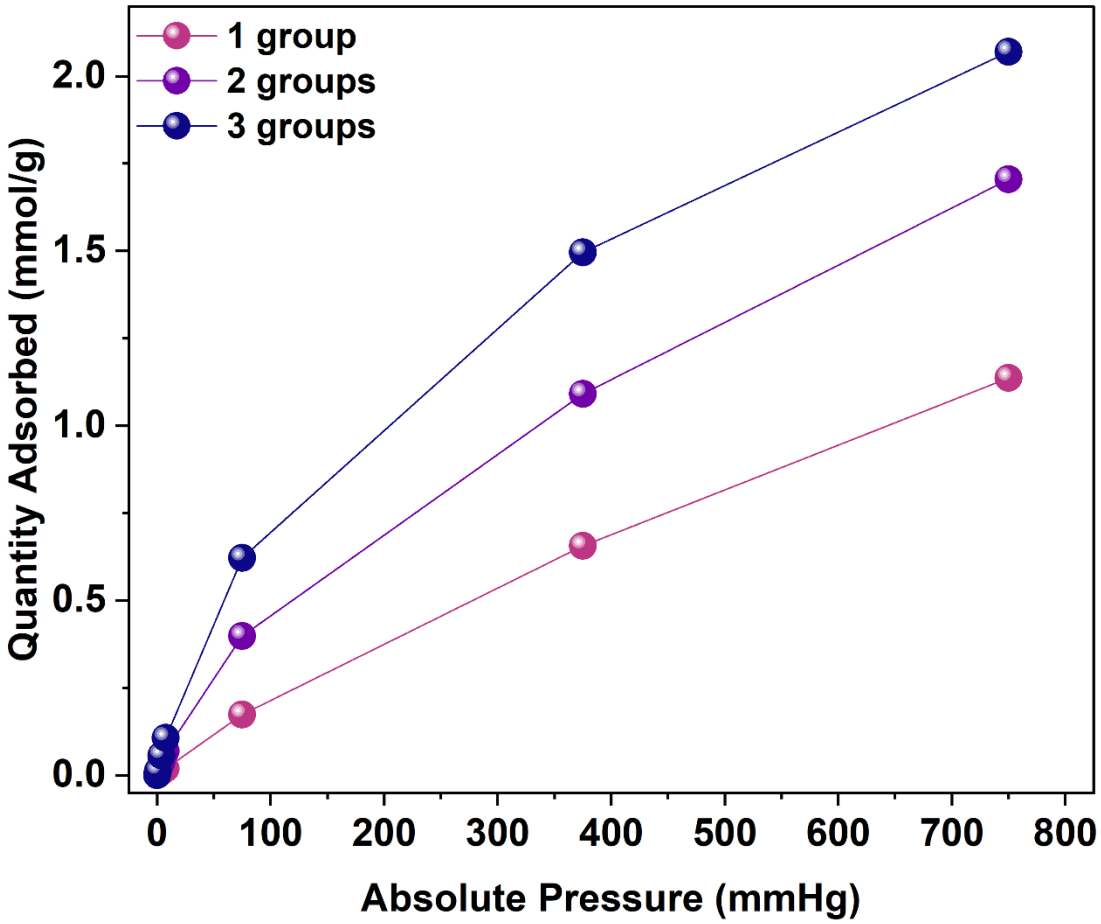

Figure S10 | Simulated SF_6 adsorption isotherms for MOF-808-CF_3 at various functional group loadings.

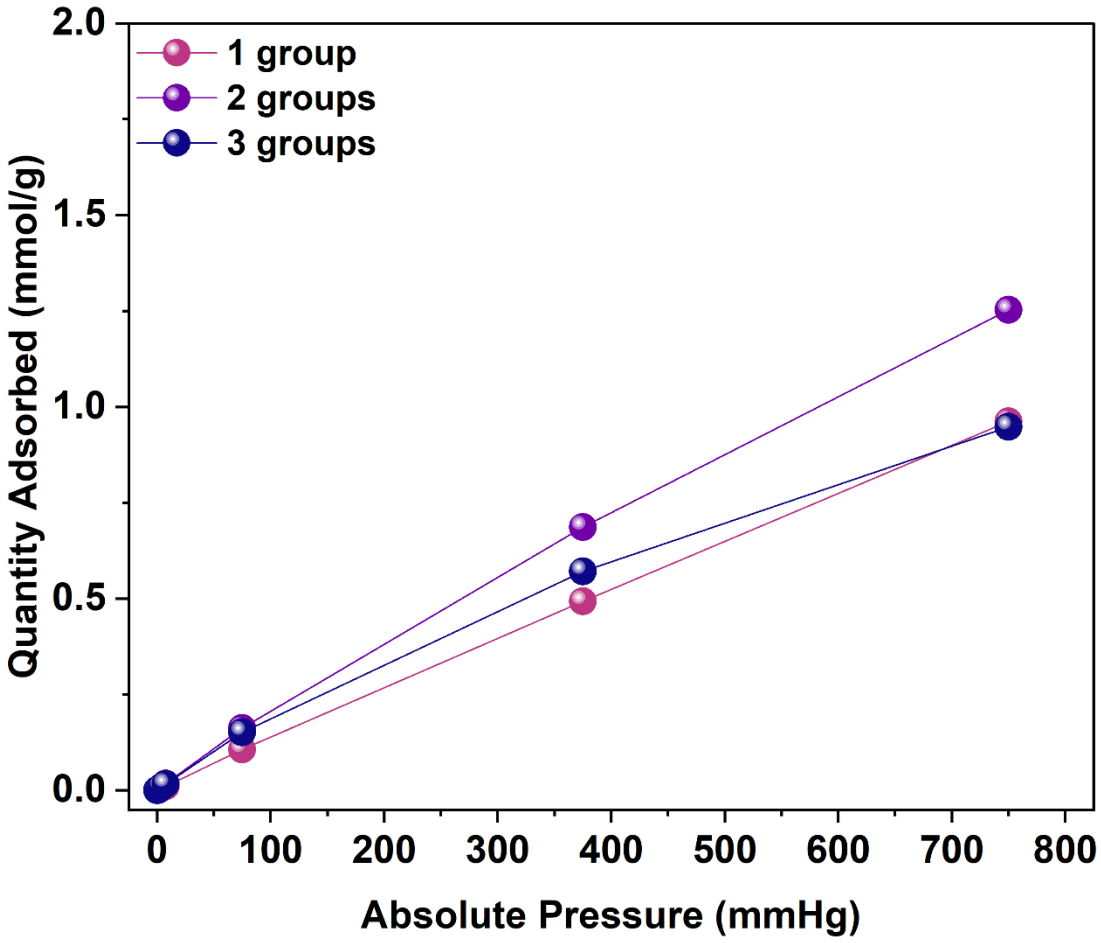

Figure S11 | Simulated SF_6 adsorption isotherms for MOF-808-$(CF_3)_2$ at various functional group loadings.

5. References

1. H. Furukawa, F. Gándara, Y.-B. Zhang, J. Jiang, W. L. Queen, M. R. Hudson and O. M. Yaghi, *Journal of the American Chemical Society*, 2014, **136**, 4369-4381.
2. R. E. Sikma, B. Song, J. I. Deneff, J. Smith, K. Sanchez, R. A. Reyes, L. M. Lucero, K. J. Fritzsching, A. G. Ilgen and D. F. S. Gallis, *Chem Commun*, 2024, **60**, 5808-5811.
3. E. A. Henle, N. Gantzler, P. K. Thallapally, X. Z. Fern and C. M. Simon, *Journal of Chemical Information and Modeling*, 2022, **62**, 423-432.
4. G. Kresse, *Physical Review B*, 1999, **59**, 1758-1775.
5. J. P. Perdew, K. Burke and M. Ernzerhof, *Physical Review Letters*, 1996, **77**, 3865-3868.
6. S. Grimme, J. Antony, S. Ehrlich and H. Krieg, *The Journal of Chemical Physics*, 2010, **132**, 154104.
7. N. G. Limas and T. A. Manz, *RSC Advances*, 2016, **6**, 45727-45747.
8. N. G. Limas and T. A. Manz, *RSC Advances*, 2018, **8**, 2678-2707.
9. T. A. Manz, *RSC Adv.*, 2017, **7**, 45552-45581.
10. T. A. Manz and N. G. Limas, *RSC Advances*, 2016, **6**, 47771-47801.
11. D. Dubbeldam, S. Calero, D. E. Ellis and R. Q. Snurr, *Molecular Simulation*, 2015, **42**, 81-101.
12. D. Dubbeldam, A. Torres-Knoop and K. S. Walton, *Molecular Simulation*, 2013, **39**, 1253-1292.

13. M. Pinheiro, R. L. Martin, C. H. Rycroft, A. Jones, E. Iglesia and M. Haranczyk, *Journal of Molecular Graphics and Modelling*, 2013, **44**, 208-219.
14. T. F. Willems, C. H. Rycroft, M. Kazi, J. C. Meza and M. Haranczyk, *Microporous and Mesoporous Materials*, 2012, **149**, 134-141.
15. A. K. Rappe, C. J. Casewit, K. S. Colwell, W. A. Goddard and W. M. Skiff, *Journal of the American Chemical Society*, 2002, **114**, 10024-10035.
16. I. Matito-Martos, J. Álvarez-Ossorio, J. J. Gutiérrez-Sevillano, M. Doblaré, A. Martin-Calvo and S. Calero, *Physical Chemistry Chemical Physics*, 2015, **17**, 18121-18130.